SCIENTIFIC REPORTS

OPEN

The synthesis, crystal, hydrogen sulfide detection and cell assement of novel chemsensors based on coumarin derivatives

Yanmei Chen[1], Xuefang Shang[1], Congshu Li[1], Zhenzhen Xue[2], Hongli Chen[3], Hongwei Wu[1] & Tianyun Wang[4]

A series of chemsensors (1–4) containing fluorobenzene group based on coumarin derivatives have been developed for the selective and sensitive detection of H_2S. The advantages of the synthesized fluorescent probe (compound 1) were the low detection limit (4×10^{-6} mol·L^{-1}), good selectivity and high sensitivity which had been demonstrated through UV-vis, fluorescent titration experiments. Besides cytotoxicity test of compounds (1 and 2) was studied and the results indicated that compounds (1 and 2) showed almost no cytotoxicityat at a concentration of 150 μg·mL^{-1}. The interacted mechanism was the thiolysis reaction of dinitrophenyl ether which had been confirmed by fluorescence and HRMS titration experiment. In addition, probe 1 can also detect HS$^-$ selectively by naked eye in pure DMSO solvent.

In the past decade, we has seen a boost of research interest in hydrogen sulfide (H₂S), a colorless, flammable, toxic gas with unpleasant smell, which is recognized as a signal gasotransmitter in the body as same as nitric oxide (NO)[1–10] and carbon monoxide (CO)[11]. Endogenous concentration of H₂S is related to some diseases such as Alzheimer's disease, Down syndrome, liver cirrhosis and diabetes[2,9,12–17]. What's more, the regulation of H₂S levels is also a potential drug development strategy[18,19] and the importance of accurate detection of H₂S cannot be over-emphasized. Therefore, it presents significant research related to track and quantify H₂S inside living cells being crucial in order to understand the biological and pathological roles of H₂S. Recently, some methods to determine H₂S concentration in biological sample have been developed including the methylene blue, the monobromobimane (MBB), gas chromatography (GC), the sulphide ion selective electrodes (ISE) and fluorescent analysis[20–23]. Among these methods, fluorescent analysis has attracted great attention due to the high sensitivity and selectivity for the detection of H₂S in many fields such as environment area, pharmacy area and so on[24–31].

In the present work, a series of "OFF-ON" probes based on coumarin derivatives to detect HS⁻ (Fig. 1). The results of UV-vis titration experiments indicated that the synthesized compounds showed high binding ability for HS⁻ among the tested anions (NaHS (HS⁻), (n-C₄H₉)₄NAcO (AcO⁻), (n-C₄H₉)₄NH₂PO₄ (H₂PO₄⁻), (n-C₄H₉)₄NF (F⁻), (n-C₄H₉)₄NCl (Cl⁻), (n-C₄H₉)₄NBr (Br⁻), (n-C₄H₉)₄NI (I⁻)) and amino acids (Glutathione (GSH), Cysteine (Cys), Homocysteine (Hcy)). Besides, four compounds designed and synthesized could exhibit the probes with strong electron-withdrawing groups located in 2,4-positions of fluorobenzene have strong binding ability for HS⁻ detection which provides a good idea for the design of probe in future.

Results and Discussion

X-ray crystallography. Compound **2** was synthesized according to the route shown in Fig. 1. Fortunately, the crystallographic of compound **2** was obtained by the standing method. The suitable single light yellow crystal was obtained by volatilizing ethyl acetate containing compound **2** at room temperature. The details of the crystallographic determination, selected bond lengths and angles were given in Table 1 and supplementary material respectively.

[1]Key Laboratory of Medical Molecular Probes, School of Basic Medical Sciences, Xinxiang Medical University, Xinxiang, Henan, 453003, China. [2]School of Pharmacy, Xinxiang Medical University, Jinsui Road 601, Xinxiang, Henan, 453003, China. [3]School of Life Sciences and Technology, Xinxiang Medical University, Jinsui Road 601, Xinxiang, Henan, 453003, China. [4]Department of biochemistry, Xinxiang Medical University, Jinsui Road 601, Xinxiang, Henan, 453003, China. Correspondence and requests for materials should be addressed to X.S. (email: xuefangshang@126.com)
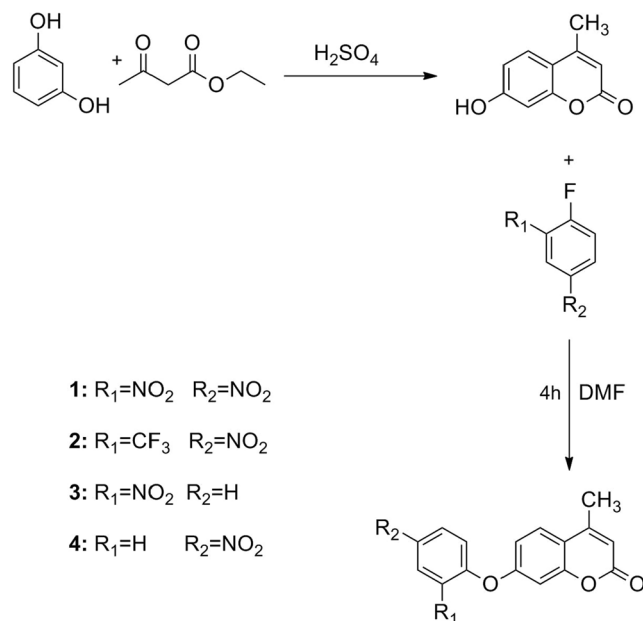
Figure 1. The synthesis route of the probes (**1**–**4**).

Compound 2	
Empirical formula	$C_{17}H_{10}F_3NO_5$
Formula Weight	365.26
Temperature	293 K
Bond precision	C-C = 0.0031 A
Wavelength	0.71073
a (Å)	7.7988(10)
b (Å)	8.2075(11)
c (Å)	13.5474(14)
α (°)	75.073(10)
β (°)	81.40(1)
γ (°)	69.207(12)
V (Å^3)	781.69(17)
Crystal system, Space group	Monoclinic, P-1
Crystal size (mm^3)	$0.45 \times 0.32 \times 0.23$
θ range for data collection (°)	3.19 to 25.01
Z	2
Mu (mm^{-1})	0.138
$F(000)$	372.0
Refinement method	Full-matrix least-squares on F^2
GOF on F^2	1.027
R_1 and wR_2 indices [$I > 2\sigma(I)$]	$R_1 = 0.0446$, w$R_2 = 0.1144$
R_1 and wR_2 indices (all data)	$R_1 = 0.0645$, w$R_2 = 0.1304$
Largest diff. peak and hole (e Å^{-3})	0.258 and -0.250

Table 1. Crystal data and structure refinement for Compound **2**.

The crystal of compound **2** suitable for X-ray crystal analysis was obtained and the structure was also confirmed (Fig. 2a). The fluoride atom in benzene cycle forms hydrogen bonds with hydrogen atom (H3) (supplementary material). The overall crystal structure features a chain type joining in through the hydrogen bonds (H….F) along the *b* axis (Fig. 2b). In the crystal packing of compound **2** (Fig. 2c), there are two stacked forms: (1) π-π stacking of one fluorobenzene ring with another; (2) π-π stacking of one coumarin ring with another, which connected into "chair" conformation along *a* axis.

UV-vis Titration. The UV-vis spectra of probes (**1**–**4**) were recorded after addition of amino acids (GSH, Cys, Hcy) and various anions (HS$^-$, AcO$^-$, H$_2$PO$_4^-$, F$^-$, Cl$^-$ Br$^-$ and I$^-$) through UV-vis titration experiments in pure
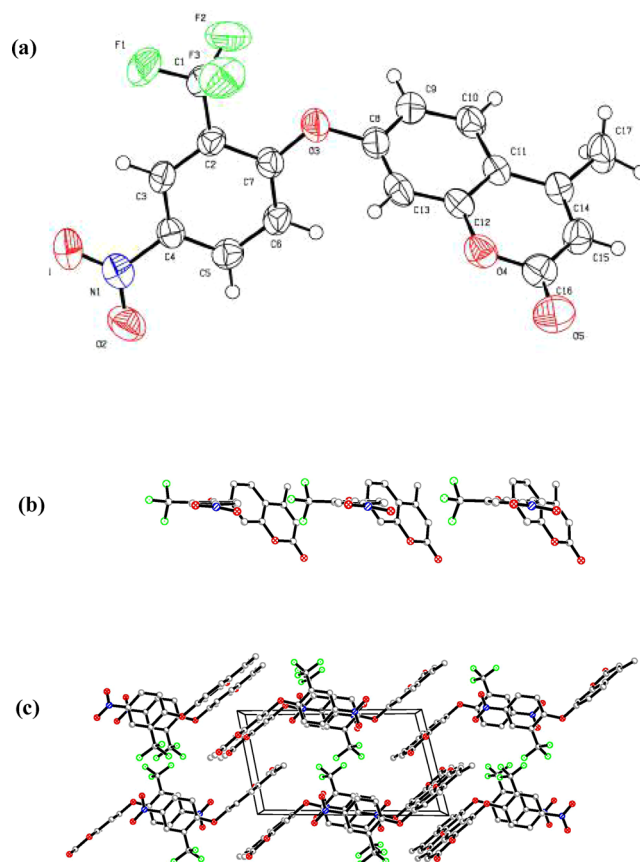
Figure 2. (**a**) The ORTEP view of compound **2** and the hydrogen atoms are shown as small circles with arbitrary radii (ellipsoids at 50% probability); (**b**) Crystal packing of compound **2** along the **b** axis; (**c**) Crystal packing of compound **2** along the *a* axis.

DMSO solution and aqueous solution (DMSO-H$_2$O 4:1, v/v 0.04 mol·L^{-1} HEPES buffer at pH 7.38) respectively. The data of UV-vis titration experiments manifested only compounds (**1**, **2**) displayed different binding abilities with the above anions and amino acids. The free **1** showed a main absorption at 320 nm, as the HS$^-$ increases in pure DMSO solution of probe **1**, the absorbance at 320 nm was decreased gradually, along with the simultaneous emergence of a new absorption at 470 nm. In this process, two isosbestic points noted at 330 nm and 348 nm suggesting a clear chemical reaction. Based on the well-establish thiolysis reaction of dinitrophenyl ether, the new absorption at 470 nm could be attributed to coumarin derivative, which was also supported by fluorescence and HRMS titration experiment. Furthermore, the UV-vis spectra of probe **1** with HS$^-$ in aqueous solution were also performed (shown in Fig. 3b), however, comparison with DMSO solvent, the probe **1** showed a weak response of UV-vis spectra.

The additions of amino acids (Cys, GSH, Hcy) and other anions (AcO$^-$, H$_2$PO$_4^-$, F$^-$, Br$^-$, Cl$^-$ and I$^-$) to pure DMSO solution of probe **1**, only Cys induced similar changes in the UV-vis spectra compared with HS$^-$, which exhibited Cys also interacted with compound **1** (supplementary material). However, the additions of the above amino acids and anions to aqueous solution induced almost no spectra changes of compound **1**. The result indicated that compound **1** showed different binding abilities for HS$^-$ and Cys in pure DMSO solution and almost no binding abilities with above amino acids and anions in aqueous solution. Therefore, compound **1** could be used as a sensor to detect HS$^-$ in aqueous solution.

Subsequently, the colorimetric sensing capabilities of compound **1** were carried out with different anions (Fig. 3c). Obvious color changes from colorless to bright yellow was observed in the presence of HS$^-$, while faint or no color changes happened in the presence of other anions (AcO$^-$, H$_2$PO$_4^-$, F$^-$, Cl$^-$, Br$^-$, I$^-$ and Cys), which indicated that compound **1** can be used for the detection of HS$^-$ as a colorimetric sensor.

Moreover, the detection limit[32,33] of compound **1** (4.0×10^{-6} mol·L^{-1}) was implemented through fluorescence titration (Fig. 3d). Further data analysis revealed an excellent linear relationship (r = 0.9963) between the fluorescence signal of the probe **1** at 392 nm and the concentration of HS$^-$ ($0-8 \times 10^{-6}$ mol·L^{-1}). Therefore, the detection limit of compound **1** for HS$^-$ was determined to be 4.0×10^{-6} mol·L^{-1}.

Next, the UV-vis titration experiments of compound **2** to various anions (HS$^-$, AcO$^-$, H$_2$PO$_4^-$, F$^-$, Br$^-$, Cl$^-$ and I$^-$) were tested. Upon the addition of increasing amounts of HS$^-$ (supplementary material) to DMSO solution of compound **2** a new absorption peak appeared gradually at 485 nm. While, the additions of other anions (AcO$^-$, H$_2$PO$_4^-$, F$^-$, Br$^-$, Cl$^-$ and I$^-$) to compound **2**, almost no spectra changes was observed.

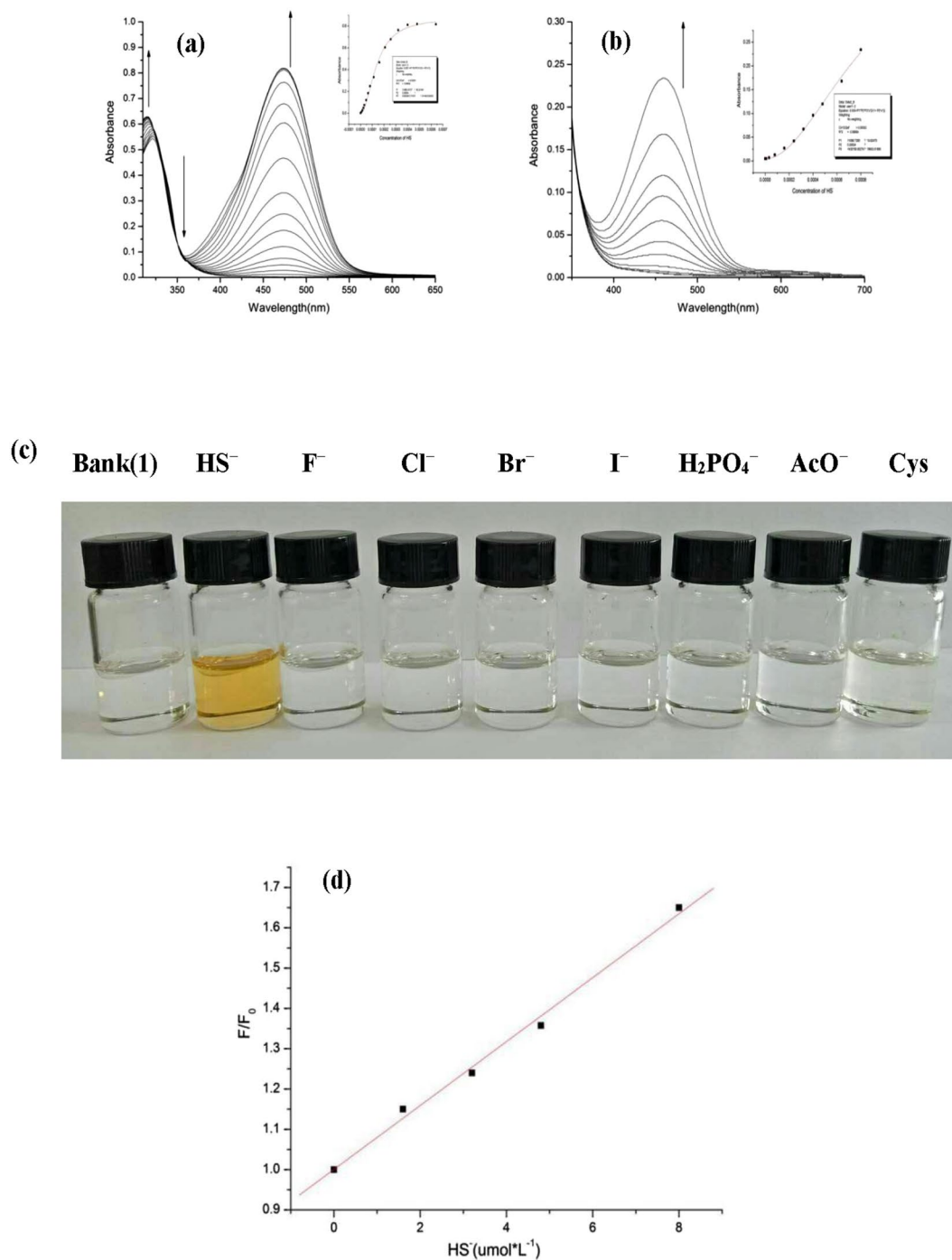**Figure 3.** UV-vis spectra of compound **1** (4.0×10^{-5} mol·L^{-1}) with the addition of HS$^-$ (0–8×10^{-6} mol·L^{-1}) (**a**) in DMSO solution; (**b**) in aqueous solution (DMSO-H$_2$O 4:1, v/v 0.04 mol·L^{-1} HEPES buffer at pH 7.38). Arrows indicate the direction of increasing HS$^-$ concentration; (**c**) Color changes observed with the addition of 20 equiv. various anions and Cys to DMSO solution of compound **1** respectively; (**d**) Fluorescent intensity of compound **1** upon the addition of HS$^-$.

Fluorescence response.   The photo-physical responses of four compounds (**1**–**4**) in DMSO solvent were also investigated with addition of various amino acids and anions. Just as Fig. 4a showed, an emission peak of free **1** exhibited at about 385 nm. Upon the addition of increasing amounts of HS$^-$, the fluorescence intensity increased obviously at about 392 nm. Similar fluorescence response of compound **1** was observed upon the addition of Cys (supplementary material) compared with HS$^-$. Furthermore, the interactions of probe **1** with amino acids (GSH, Hcy) and other anions (AcO$^-$, H$_2$PO$_4^-$, F$^-$, Br$^-$, Cl$^-$ and I$^-$) were also investigated. The additions of H$_2$PO$_4^-$, AcO$^-$ and F$^-$ (supplementary material) induced the appearance of fluorescence emission bands centered at about 386 nm, however, nominal changes were induced in the presence of GSH, Hcy, F$^-$, Cl$^-$, Br$^-$, I$^-$.
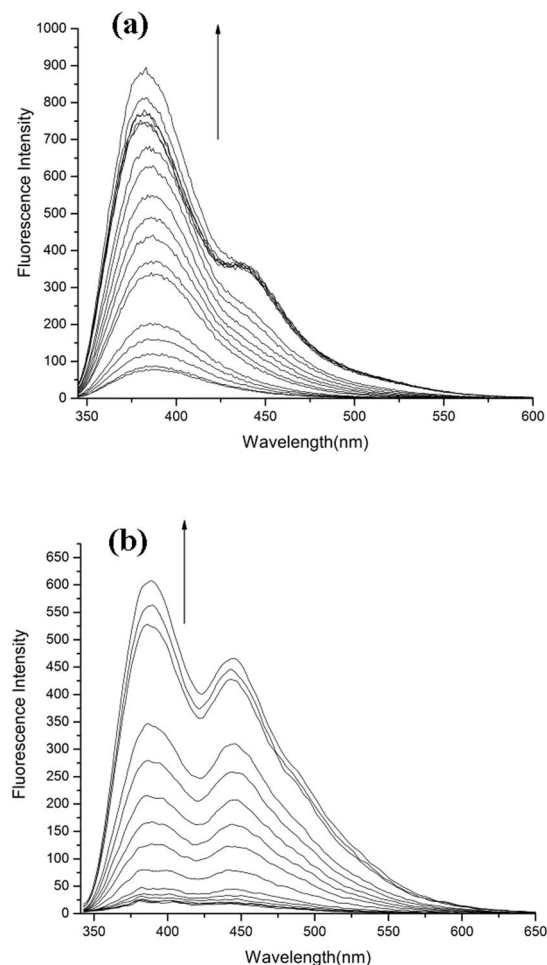
Figure 4. Fluorescence responses (λ_{ex} 331 nm, slit widths: 5 nm/5 nm) of compound **1** (4.0×10^{-5} mol. L^{-1}) upon the additions of HS^- (**a**) in pure DMSO solution; (**b**) in aqueous solution (DMSO-H_2O 4:1, v/v 0.04 mol·L^{-1} HEPES buffer at pH 7.38). Arrows indicate the increasing concentration of HS^-.

Besides, the fluorescence spectral responses of compound **1** with amino acids (Cys, GSH, Hcy) and various anions (HS^-, AcO^-, $H_2PO_4^-$, F^-, Br^-, Cl^- and I^-) were also examined in aqueous solution. From Fig. 4b, compound **1** showed very weak fluorescence at the absence of anions. After HS^- was added, double emission peaks appeared and the fluorescent intensity increased gradually. Results demonstrated that compound **1** showed strong binding ability for HS^-. However, weak spectral responses that even could be ignored were induced with addition of amino acids (Cys, GSH, Hcy) and $H_2PO_4^-$, AcO^-, F^-, Cl^-, Br^-, I^-.

For compound **2**, the fluorescence intensity noted at 434 nm increasing rapidly by titration of HS^- (supplementary material). No obvious responses of compound **2** were observed with titration of other anions (AcO^-, $H_2PO_4^-$, F^-, Br^-, Cl^- and I^-) and Cys. For compounds (**3** and **4**), Similar experiments were carried out, however, no significant spectral responses were observed with the addition of other anions (HS^-, $H_2PO_4^-$, AcO^-, F^-, Br^-, Cl^- and I^-) into DMSO solution of two compounds (**3** and **4**) which indicated the weak binding abilities of compounds (**3** and **4**) and other anions (AcO^-, $H_2PO_4^-$, F^-, Br^-, Cl^- and I^-) and Cys could be ignored.

Binding constant. The job-pot curves suggested two compounds (**1** and **2**) interacted with amino acids and various anions as the ratio of 1:1 or 1:2. The UV-vis spectral data was used to calculate the binding constants by non-linear least square method[34,35], and the binding constants were listed in the Table 2. Obviously, the binding ability of two compounds (**1** and **2**) with amino acids and various anions followed the order of $HS^- \gg H_2PO_4^-$, Cys, AcO^-, F^-, Br^-, Cl^-, I^-, Hcy and GSH. In general, both compound **1** and compound **2** showed the strongest binding ability for HS^- among amino acids and anions. Besides, a theoretical basis and these binding constants were necessary for the optimization of sensor.

The anion binding abilities of compounds (**1** and **2**) with two electron-withdrawing groups on the fluorobenzene ring were stronger than that of compounds (**3** and **4**) which had one electron-withdrawing group on the fluorobenzene ring. In addition, the anion binding ability of compound **1** was stronger than that of compound **2** due to the electron-withdrawing ability of nitro group was greater than the trifluoromethyl group[36]. The above results indicated that strong electron-withdrawing groups located in 2, 4-positions of fluorobenzene provides a

Anion	Compound 1 (DMSO)	Compound 1 (DMSO:HEPES = 4:1)	Compound 2 (DMSO)
HS$^-$	$(5.32 \pm 0.08) \times 10^{7b}$	$(1.43 \pm 0.07) \times 10^{6b}$	$(33.9 \pm 0.8)^a$
Cys	$(7.91 \pm 0.64) \times 10^{3a}$	ND	ND
AcO$^-$	ND	ND	ND
F$^-$	ND	ND	ND
H$_2$PO$_4^-$	ND	ND	ND
Cl$^-$ Br$^-$ or I$^-$	ND	ND	ND

Table 2. Binding constants of compound (**1** and **2**) with various anions. [a]The binding ratio of host-guest is 1:1. [b]The binding ratio of host-guest is 1:2.

easily site for intermolecular HS$^-$ attack. Besides, for HS$^-$, the binding ability trend of compounds (**1–4**) followed the order of **1** > **2** ≫ **3**, **4** also could be confirmed by comprehensive analysis of UV-vis, fluorescence titration.

Mechanism. The interacted mechanism was measured by fluorescence and HRMS titration experiment. The broad emission peak of compound **1** appeared at about 396 nm in the absence of HS$^-$. The emission peak shifted to the short wavelength from 396 nm to 380 nm after HS$^-$ was added. The emission peak of the single 7-hydroxy-4-methylcoumarin appeared at about 380 nm. The same emission peak observed in the presence of HS$^-$ which suggested free 7-hydroxy-4-methylcoumarin was released after compound **1** interacted with HS$^-$ (Fig. 5a). Furthermore, the interacted mechanism of host-guest (**1**-HS$^-$) was also carried by performing MS-HRMS after the addition of 2 equiv. NaHS. The probe **1** itself exhibited a dominant peak at m/z = 341.0551(*M*-H)$^-$ (supplementary material). However, the above peak vanished and a new peak at m/z = 199.0364 (*M* + Na)$^+$ appeared which was the ion-peak of 7-hydroxy-4-methylcoumarin (Fig. 5b) after the addition of HS$^-$. The MS-HRMS titration experiment suggested the binding ratio of host-guest (**1**-HS$^-$) was 1:2. The above results indicated the possible interacted mechanism was thiolysis reaction of dinitrophenyl ether (Fig. 5c)[37–44].

Cytotoxicity Assay. For further biological application point of view, a quantitative cytotoxicity study of two compounds (**1** and **2**) *in vitro* was conducted using MTT assay. Owning to Glutathione peroxidase (GPx1) being an important selenoprotein and not found in human breast cancer cells (MCF-7) according to scientific research, therefore, the special cell lines (MCF-7 cell) were selected by us[45,46]. The MTT assay results indicated that compound **1** and **2** showed very low cotoxicity over a concentration range of 0–150 μg·mL^{-1} especial probe **2** (Fig. 6). Cellular viability was minimally affected (80%, cellular viability) with the compounds (**1** and **2**) (<150 μg·mL^{-1}). In agreement with the binding constants, compounds (**1** and **2**) showed a high binding capacity and low cytotoxicity, especial probe **1**, which indicated that compounds (**1** and **2**) have a potential application to H$_2$S detection in cells.

Material and Methods

Most staring materials were obtained commercially, all reagents and solvents were of analytical grade and used as received without further purification unless otherwise stated. Sodium hydrolfide and all anions in the form of tetrabutylammonium salts (such as (*n*-C$_4$H$_9$)$_4$NCl, (*n*-C$_4$H$_9$)$_4$NBr, (*n*-C$_4$H$_9$)$_4$NI, (*n*-C$_4$H$_9$)$_4$NAcO and (*n*-C$_4$H$_9$)$_4$NH$_2$PO$_4$) and amino acides (Cys, GSH and Hcy) were purchased from Aladdin Chemistry Co. Ltd (Shanghai, China). Dimethyl sulfoxide (DMSO) was distilled in vacuum after being dried with CaH$_2$. 1H NMR spectra were recorded using an Unity Plus-400-MHz spectrometer. HRMS was obtaioned with a Mariner apparatus. Absorption spectra were obtained on UV-vis spectrophotometer (Shimadzu, UV-2600, Japan). Fluorescence emmission spectra were taken on a Cary Eclipse Fluorescence Spectrophotometer (Agilent, USA). The binding constant (K_s) was obtained by non-linear least squares calculation method for data fitting.

The cells that were at logarithmic growth phase were seeded in a 96-well plate at a density of 2.0×10^4 cell peer well for 24 h, followed by treatment different concentration of compound at 37 °C for additional 24 h. Next, cells were collected and washed with PBS three times then 100 μL of culture medium and 20 μL of MTT solution were added to each well respectively, and the cells were incubated for 4 h. The absorbance were detected by microplate reader (Thermo Multiscan MK3, Thermo Fisher Scientific, MA, USA) at 490 nm wavelength measurement. Cell viability (expressed in%) was calculated considering 100% growth at the absence of fluorescence probe, and the viability of other groups were calculated by comparing the optical density reading with the control. The IC50 was defined as the compound concentrations required for 80% inhibition of cell growth.

Synthesis of the probes. The compounds (**1–4**) were synthesized according to the route shown in Fig. 1.

Synthesis of 7-hydroxy-4-methylcoumarin (1). 7-Hydroxy-4-methylcoumarin was synthesized according to the literature[47]. The experimental details were described in supplementary material.

Synthesis of compound 1. 7-Hydroxy-4-methyl coumarin (2.16 g, 12 mmol) and 2,4-dinitrofluorobenzene (1.5 g, 8 mmol), K$_2$CO$_3$ (3.39 g, 24 mmol) were dissolved in DMF(40 mL) solution with stirring. The above mixture were heated for 4 h at 90 °C at N$_2$ atmosphere and then cooled to room temperature. The reaction was poured into
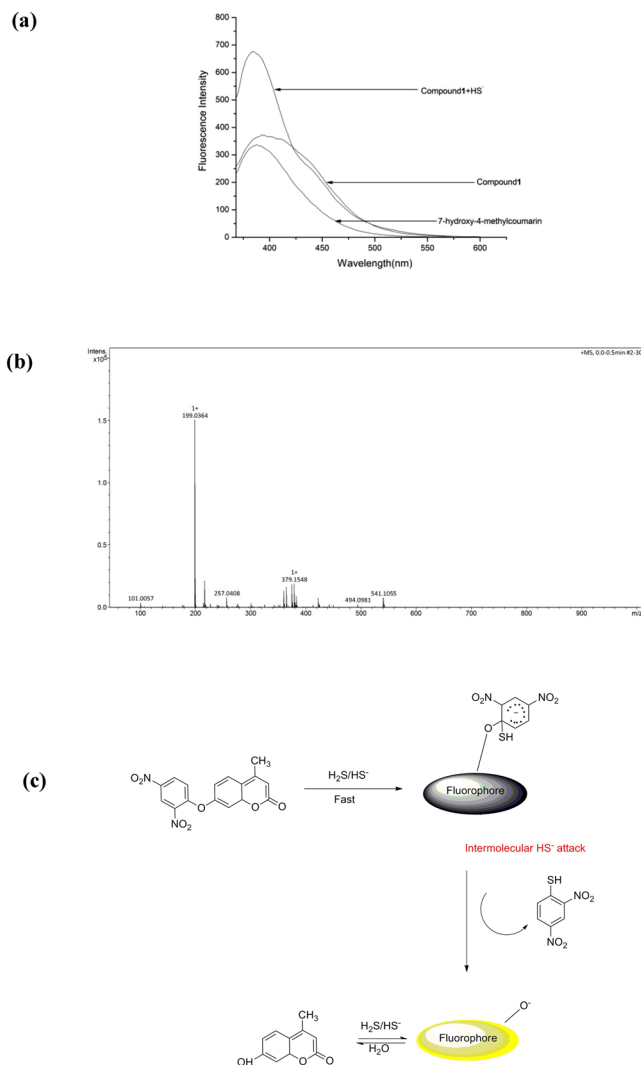
Figure 5. (**a**) A comparison of fluorescence spectra in the presence of 3.2 equiv HS$^-$ between compound **1** and 7-hydroxy-4-methylcoumarin (4.0×10^{-5} mol·L^{-1}); (**b**) ESI-HRMS spectrum of compound **2** after addition of 2 equiv of NaHS in DMSO solution. MS-HRMS (m/z): 199.0364 ($M + $Na)$^+$; (**c**) The possible interacted mechanism of host-guest.
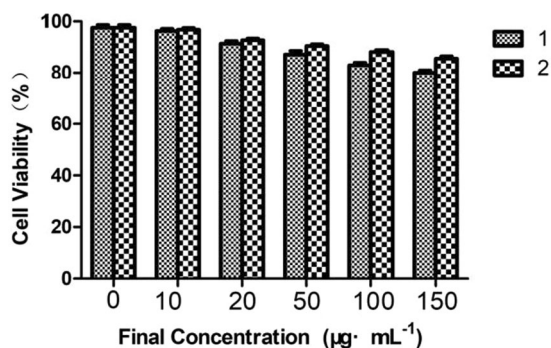

Figure 6. Cell viabilities were measured by MTT assay after 24 h in the presence of of fluorescence probe (0–150 μg·mL^{-1}) incubation. Cell viability (expressed in%) was set as 100% growth in the absence of fluorescence probe.

ice-water (400 mL) and extracted with ethyl acetate (3×25 mL), dried with MgSO$_4$ overnight. Filtration, purification with column chromatography (CH$_3$COOCH$_2$CH$_3$:CH$_2$Cl$_2$ = 1:40). Stood overnight a yellow precipitate was obtained. Yield: 68%. m.p. 187.9–189.8 °C. ^{1}H NMR (400 MHz, DMSO-d_6) δ 8.94 (s, 1 H), 8.51 (dd, $J = 9.2, 2.8$ Hz,

1 H), 7.92 (d, $J = 8.7$ Hz, 1 H), 7.40 (dd, $J = 15.6$, 5.8 Hz, 2 H), 7.28 (dd, $J = 8.7$, 2.5 Hz, 1 H), 6.43 (s, 1 H), 2.47 (s, 3 H) (supplementary material). Elemental analysis: Calc. for $C_{16}H_{10}N_2O_7$: C, 56.15; H, 2.94; N, 8.18. Found: C, 56.21; H, 2.94; N, 8.16. MS-HRMS (m/z): 341.0551(M-H)- (supplementary material). IR: C-O-C (Diphenyl oxide Phenyl ether Biphenyloxide): 1288 cm^{-1} (supplementary material).

Compounds (**2**–**4**) were also synthesized according to the above similar procedure.

Compound 2.   Suitable single light yellow crystal for X-ray crystal structure analysis was obtained. Yield: 74%. m.p. 139.3–142.1 °C. ^{1}H NMR (400 MHz, DMSO-d_6) δ 8.56 (d, $J = 2.8$ Hz, 1 H), 8.51 (dd, $J = 9.1$, 2.8 Hz, 1 H), 7.91 (d, $J = 8.7$ Hz, 1 H), 7.39–7.30 (m, 2 H), 7.23 (dd, $J = 8.7$, 2.5 Hz, 1 H), 6.42 (s, 1 H), 2.46 (s, 3 H) (supplementary material). Elemental analysis: Calc. for $C_{17}H_{10}FNO_5$: C, 55.90; H, 2.76; N, 3.83. Found: C, 55.83; H, 2.76; N, 3.84. MS-HRMS (m/z): 366.0589($M + H$)$^+$ (supplementary material). IR: C-O-C (Diphenyl oxide Phenyl ether Biphenyloxide): 1274 cm^{-1} (supplementary material).

Compound 3.   Yield: 75%. m.p. 140.9–143.6 °C. ^{1}H NMR (400 MHz, DMSO-d_6) δ 8.16 (dd, $J = 8.2$, 1.5 Hz, 1 H), 7.86–7.76 (m, 2 H), 7.51 (t, $J = 7.8$ Hz, 1 H), 7.39 (d, $J = 8.3$ Hz, 1 H), 7.09–7.01 (m, 2 H), 6.35 (s, 1 H), 2.43 (s, 3 H) (supplementary material). Elemental analysis: Calc. for $C_{16}H_{11}NO_5$: C, 64.65; H, 3.73; N, 4.71. Found: C, 64.72; H, 3.72; N, 4.72. MS-HRMS (m/z): 320.0550($M + Na$)$^+$ (supplementary material). IR: C-O-C (Diphenyl oxide Phenyl ether Biphenyloxide): 1273 cm^{-1} (supplementary material).

Compound 4.   Yield: 78%. m.p. 165.5–167.3°C. ^{1}H NMR (400 MHz, DMSO-d_6) δ 8.35–8.27 (m, 2 H), 7.88 (d, $J = 8.7$ Hz, 1 H), 7.28 (dd, $J = 10.2$, 3.1 Hz, 3 H), 7.19 (dd, $J = 8.7$, 2.4 Hz, 1 H), 6.40 (s, 1 H), 2.46 (s, 3 H) (supplementary material). Elemental analysis: Calc. for $C_{16}H_{11}NO_5$: C, 64.65; H, 3.73; N, 4.71. Found: C, 64.82; H, 3.74; N, 4.70. MS-HRMS (m/z): 320.0533 ($M + Na$)$^+$ (supplementary material). IR: C-O-C (Diphenyl oxide Phenyl ether Biphenyloxide): 1267 cm-1 (supplementary material).

A light yellow crystal of compound **2** with dimensions of 0.45 nm × 0.32 nm × 0.23 nm was mounted on a glass fiber. X-ray single-crystal diffraction data was collected on a Rigaku saturn CCD area detector at 293 K with Mo-Ka radiation (λ = 0.71073 Å). The structure was solved by direct methods and refined on F^2 by full-matrix least squares methods with SHELXL-97[48].

Conclusion

In conclusion, we developed a series of fluorescence probes based on coumarin derivatives for the detection of H_2S successively with OFF-ON" fluorescence response. The fluorescence probes, especially compound **1**, exhibited remarkable response to H_2S against other anions and amino acids in pure DMSO solvent. Otherwise, the probe **1** also showed strong binding ability for HS$^-$ in HEPES buffer solution. The interacted mechanism of host-guest was the thiolysis reaction of dinitrophenyl ether. In addition, compound (**1 and 2**) showed highly sensitivity and low cytotoxicity to MCF-7 cells and probe **1** can also detect HS$^-$ selectively by naked eye in pure DMSO solvent. The results of our efforts highlight that the probes, especially compound **1**, hold a potential chemical tool for the detection of H_2S.

References

1. Yu, H., Xiao, Y. & Jin, L. A lysosome-targetable and two-photon fluorescent probe for monitoring endogenous and exogenous nitric oxide in living cells. *J. Am. Chem. Soc.* **134**, 17486–17489 (2012).
2. Szabó, C. Hydrogen sulfide and its therapeutic potential. *Nat. Rev. Drug. Discov.* **6**, 917–935 (2007).
3. Li, L., Rose, P. & Moore, P. K. Hydrogen sulfide and cell signaling. *Ann Rev Pharmacol Toxicol.* **51**, 169–187 (2011).
4. Predmore, B. L., Lefer, D. J. & Gojon, G. Hydrogen Sulfide in Biochemistry and Medicine. *Antioxid Redox Signaling.* **17**, 119–140 (2012).
5. Yang, G. *et al*. H$_2$S as a Physiologic Vasorelaxant: Hypertension in Mice with Deletion of Cystathionine γ-lyase. *Science.* **322**, 587–590 (2008).
6. Kimura, H. Hydrogen sulfide:its production, release and functions. *Amino Acides.* **41**, 113–121 (2011).
7. Whiteman, M. & Moore, P. K. Hydrogen sulfide and the vasculature:a novel vasculoprotective entity and regulator of nitric oxide bioavailability. *J. Cell. Mol. Med.* **13**, 488–507 (2009).
8. Kimura, H. Hydrogen sulfide:its production and fuctions. *Exp. Physiol.* **96**, 833–835 (2011).
9. Gadalla, M. M. & Snyder, S. H. Hydrogen sulfide as a gasotransmitter. *J. Neurochem.* **113**, 14–26 (2010).
10. Sen, N. *et al*. Hydrogen sulfide-linked sulfhydration of NF-κB mediates its antiapoptotic actions. *Mol. Cell.* **45**, 13–14 (2012).
11. Hong, P. K., Ryter, S. W. & Choi, A. M. K. CO as a cellular signaling molecule. *Annu. Rev. Pharmacol.* **46**, 411–449 (2006).
12. Kamoun, P., Belardinelli, M.-C., Chabli, A., Lallouchi, K. & Chadefaux-Vekemans, B. Endogenous hydrogen sulfide overproduction in down syndrom. *Am. J. Med. Genet.* **116**, 310–311 (2003).
13. Takano, Y., Shimamoto, K. & Hanaoka, K. Chemical tools for the study of hydrogen sulfide (H$_2$S) and sulfane sulfur and their applications to biological studies. *J. Clin. Biochem. Nutr.* **58**, 7–15 (2016).
14. Yan, Y. *et al*. Sensitive detection of sulfide based on the self-assembly of fluorescent silver nanoclusters on the surface of silica nanospheres. *Talant.* **174**, 387–393 (2017).
15. Eto, K. *et al*. Brain hydrogen sulfide is severely decreased in Alzheimer's disease. *Bio. Chem. Bioph. Res. Co.* **293**, 1485–1488 (2002).
16. Kashfi, K. The role of hydrogen sulfide in health and disease. *Biochem. Pharmacol.* **149**, 1–4 (2018).
17. Cao, X. *et al*. The role of hydrogen sulfide in cyclic nucleotide signaling. *Biochem. Pharmacol.* **149**, 20–28 (2018).
18. Martelli, A. *et al*. Hydrogen sulphide: novel opportunity for drug discovery. *Med. Res. Rev.* **32**, 1093–1130 (2012).
19. Vandiver, M. S. & Snyder, S. H. Hydrogen sulfide: a gasotransmitter of clinical relevance. *J. M. M.* **90**, 255–263 (2012).
20. Li, H. *et al*. Simultaneous removal and measurement of sulfide on the basis of turn-on fluorimetry. *Int. J. Environ. Sci. Technol*., https://doi.org/10.1007/s13762-017-1483-z (2017).
21. Hughes, M. N., Centelles, M. N. & Moore, K. P. Making and working with hydrogen sulfide: The chemistry and generation of hydrogen sulfide *in vitro* and its measurement *in vivo. a review. Free Radicals Biol. Med.* **47**, 1346–1353 (2009).
22. Shen, X. G. *et al*. Measurement of plasma hydrogen sulfide *in vivo* and *in vitro*. *Free Radicals Biol. Med.* **50**, 1021–1031 (2011).
23. Chen, Y. M. *et al*. Highly selective probes of copper(II) complexes for sulfide detection and cytotoxicity assay. *J. Sulfur Chem.* **39**, 308–321 (2018).

24. Thomas, S. C., Samuel, M. R. & Xue, Z. L. Quantitative, colorimetric paper probe for hydrogen sulfide gas. *Sensors Actuat. B-Chem.* **253**, 846–851 (2017).
25. Xu, Q. C., Gu, Z. Y. & Xing, G. W. Design and synthesis of a Cu(II)-complex-based carbazole-hemicyanine hybrid for fluorescent sensing of H₂S in SDS micellar solution. *Tetrahedron.* **73**, 2123–2130 (2017).
26. Zhang, D. & Jin, W. Highly selective and sensitive colorimetric probe for hydrogen sulfide by a copper (II) complex of azo-dye based on chemosensing ensemble approach. *Spectrochim Acta. A.* **90**, 35–39 (2012).
27. Sun, M. *et al.* Fluorescence signaling of hydrogen sulfide in broad pH range using a copper complex based on BINOL-benzimidazole ligands. *Inorg. Chem.* **54**, 3766–3772 (2015).
28. Ding, S., Feng, W. & Feng, G. Rapid and highly selective detection of H2S by nitrobenzofurazan (NBD) ether-based fluorescent probes with an aldehyde group. *Sensors Actuat. B-Chem.* **238**, 619–625 (2016).
29. Park, C. S. *et al.* A near-infrared "turn-on" fluorescent probe with a self-immolative linker for the *in vivo* quantitative detection and imaging of hydrogen sulfide. *Biosens. Bioelectron.* **89**, 919–92 (2016).
30. Ryu, H. G. *et al.* Two-photon fluorescent probe for hydrogen sulfide based on a red-emitting benzocoumarin dye. *Tetrahedron Lett.* **59**, 49–53 (2018).
31. Fei, Q. *et al.* Design of BODIPY-based near-infrared fluorescent probes for H2S. *J. Photoch. Photobio. A.* **355**, 305–310 (2017).
32. Zhu, M. *et al.* Visible near-infrared chemosensor for mercury ion. *Org. Lett.* **10**, 1481–1484 (2008).
33. Isaad, J. & Achari, A. E. Biosourced 3-formyl chromenyl-azo dye as Michael acceptor type of chemodosimeter for cyanide in aqueous environment. *Tetrahedron.* **67**, 5678–85 (2011).
34. Liu, Y., You, C. C. & Zhang, H. Y. *Supramolecular Chemistry*., (Nankai University Publication, Tianjin, 2001).
35. Bourson, J., Pouget, J. & Valeur, B. Ion-responsive fluorescent compounds. 4. Effect of cation binding on the photophysical properties of a coumarin linked to monoaza- and diaza-crown ethers. *J. Phys. Chem.,* **97**, 4552–4557 (1993).
36. Hansch, C., Leo, A. & Taft, R. W. A Survey of Hammett Substituent Constants and Resonance and Field Parameters. *Chem. Rev.* **97**, 165–195 (1991).
37. Das, A. K. *et al.* Neighbouring group participation of thiol through aldehyde group assisted thiolysis of active ether: ratiometric and vapor phase fast detection of hydrogen sulfide in mixed aqueous media. *New J. Chem.* **39**, 5669–5675 (2015).
38. Huang, Z. *et al.* Aldehyde group assisted thiolysis of dinitrophenyl ether: a new promising approach for efficient hydrogen sulfide probes. *Chem. Commun.* **50**, 9185–9187 (2014).
39. Liu, T. *et al.* A lysosome-targetable fluorescent probe for imaging hydrogen sulfide in living cells. *Org. Lett.* **15**, 2310–2313 (2013).
40. Zheng, K. *et al.* A two-photon fluorescent probe with a large turn-on signal for imaging hydrogen sulfide in living tissues. *Anal. Chim. Acta.* **853**, 548–554 (2015).
41. Zhang, C. *et al.* A FRET-ICT dual-quenching fluorescent probe with large off-on response for H2S: synthesis, spectra and bioimaging. *Chem. Commun.* **51**, 7505–7508 (2015).
42. Wang, J. *et al.* A BODIPY-based turn-on fluorescent probe for the selective detection of hydrogen sulfide in solution and in cells. *Talanta.* **144**, 763–768 (2015).
43. Zhao, Q. *et al.* "Turn-on" fluorescent probe for detection of H2S and its applications in bioimaging. *S.A.P:M&B.S.* **189**, 8–12 (2018).
44. Chen, Q. *et al.* Sensitive and rapid detection of endogenous hydrogen sulfide distributing in different mouse viscera *via* a two-photon fluorescent probe. *Anal. Chim. Acta.* **896**, 128–136 (2015).
45. Vibet, S. *et al.* Sensitization by docosahexaenoic acid (DHA) of breast cancer cells to anthracyclines through loss of glutathione peroxidase (GPx1) response. *Free Radical Bio. Med.* **44**, 1483–1491 (2008).
46. Shang, X. *et al.* Development and cytotoxicity of Schiff base derivative as a fluorescence probe for the detection of L-Arginine. *J. Mol. Struct.* **1134**, 369–373 (2017).
47. Ahluwalia, V. K., Bhagat, P., Aggarwal, R. & Chandra, R. Intermediates for Organic Synthesis, I. K. International Pvt. Ltd, Delhi (2005).
48. Sheldrick G. M. SHELX97. Programs for crystal structure analysis. University of Gottingen, Germany (1997).

Acknowledgements

Author Contributions

X.S., H.W., T.W. directed the work. Y.C. conceived the idea and designed the experiments. Y.C. and Z.X. performed the synthesis. C.L., H.C. performed the cytotoxicity Assay. Y.C. wrote the manuscript. All authors reviewed the manuscript.

Additional Information

Supplementary information accompanies this paper at https://doi.org/10.1038/s41598-018-34331-9.

Competing Interests: The authors declare no competing interests.

Publisher's note: Springer Nature remains neutral with regard to jurisdictional claims in published maps and institutional affiliations.